Article

Catalytic Steam Reforming of Toluene: Understanding the Influence of the Main Reaction Parameters over a Reference Catalyst

Hua Lun Zhu, Laura Pastor-Pérez and **Marcos Millan** *

Department of Chemical Engineering, Imperial College London, London SW7 2AZ, UK;
h.zhu16@imperial.ac.uk (H.L.Z.); l.pastor-perez@imperial.ac.uk (L.P.-P.)
* Correspondence: marcos.millan@imperial.ac.uk

check for updates

Abstract: Identifying the suitable reaction conditions is key to achieve high performance and economic efficiency in any catalytic process. In this study, the catalytic performance of a Ni/Al_2O_3 catalyst, a benchmark system—was investigated in steam reforming of toluene as a biomass gasification tar model compound to explore the effect of reforming temperature, steam to carbon (S/C) ratio and residence time on toluene conversion and gas products. An S/C molar ratio range from one to three and temperature range from 700 to 900 °C was selected according to thermodynamic equilibrium calculations, and gas hourly space velocity (GHSV) was varied from 30,600 to 122,400 h^{-1} based on previous work. The results suggest that 800 °C, GHSV 61,200 h^{-1} and S/C ratio 3 provide favourable operating conditions for steam reforming of toluene in order to get high toluene conversion and hydrogen productivity, achieving a toluene to gas conversion of 94% and H_2 production of 13 mol/mol toluene.

1. Introduction

Greenhouse gas (GHG) emissions from fossil fuel combustion for power generation represent a major contribution to climate change. For this very reason, a switch from conventional to renewable power resources, i.e., solar, wind, hydroelectric energy and biomass is necessary [1].

Biomass can consistently provide energy and fuels and has an advantage over other renewable energies sources as it is more homogeneously distributed over the earth and is an abundant resource [2]. International Energy Outlook 2017 reported that biomass could provide over 14% of the world's primary energy consumption, which is the highest among renewable energy resource, and it will contribute a quarter or third of the global primary energy supply by 2050 [3].

For all the above and as a consequence of unstable oil prices and the alarming climate change, biomass gasification has increasingly received interest [4]. Indeed, this is a versatile and interesting way to re-use different wastes (e.g., agricultural and urban wastes, energy crops, food and industrial processing residues) to produce bio-syngas, which can be used for electrical power generation (fuel cells, gas turbine or engine), or as feedstock for the synthesis of liquid fuels and chemicals such as methanol [5]. Furthermore, the necessary technology for this process can be adapted from old coal gasification units [6]. However, one of the most critical technical challenges in biomass gasification is the formation of tars. Tar condensation can cause serious risks to downstream equipment. Therefore, tars should be removed from the effluent stream of biomass gasification [7].

Existing techniques for tar removal after a gasifier include separation either by physical (mechanical) methods, using ceramic candle filters or wet scrubbers, or thermochemical conversion

methods using high temperature thermal or catalytic cracking to convert tar into syngas [8]. Physical separation methods would cause secondary pollution since they only remove tar from gas products, resulting in a waste stream that needs treatment. Conversely, thermal cracking has received increasing attention because tar can be converted into useful gas products and increases the overall efficiency of the gasification process [9]. Thermal cracking without catalysts operates at high temperature (>1000 °C) to decompose the tars in smaller non-condensable molecules. The high energy consumption makes this process less interesting. By contrast, catalytic cracking of tars can be carried out at lower temperatures converting tars into useful gases in a more efficient manner and is being widely studied as a principal method for tar removal [10]. As a steam reforming reaction, the proposed reaction could remove tar by a catalytic process and produce fuel H_2 and CO at relatively low temperatures. At the same time, tar steam reforming poses some challenges that must be addressed related to the reaction conditions. Reforming catalysts can lose activity over time due to carbon deposition and sintering over the active phases [5]. These problems can be minimised with optimal operating conditions in the presence of the right catalyst. Real tar composition is highly complex and most studies use model tar compounds such as toluene, benzene or naphthalene to ascertain the catalytic mechanism [11–13]. However, previous studies have shown that these compounds represent a worst-case scenario in the tendency of the system to form carbon deposits [14,15].

Noble metals and Ni are most widely active phases used in reforming catalysts. Noble metal catalysts including Pt, Rh and Ru are known for their exceptionally good activity and stability in tar steam reforming. However, these catalysts have had limited use due to their high costs [16].
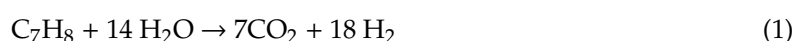
Nowadays, the aim is to develop an economically viable material, ideally not containing noble metals, which produces the same high levels of conversion and reaction performance as the noble ones. Ni is an attractive choice as steam reforming catalytic metal thanks to its good performance in the conversion of different types of hydrocarbons [16], being, for instance, the most popular active phase in methane steam reforming [17,18]. In particular, Ni/Al_2O_3 catalysts are considered as the state-of-the-art materials for steam reforming processes. Furthermore, the high surface area of alumina and its mechanical properties result in an excellent choice as support for nickel nanoparticles [19].

Under these premises, this work showcases the application of a Ni/Al_2O_3 catalyst in the steam reforming of toluene (C_7H_8) as a tar model compound in a fixed bed reactor. Until now, the catalytic performance in the steam reforming of toluene has been mainly evaluated as a function of catalyst design variables, such as the nature of the support [20–22] and metal [23,24], but little attention has been paid to the reaction conditions, especially for this benchmark catalytic formulation [25]. Identification and optimisation of the reaction parameters in the presence of a commercial-like catalyst (Ni/Al_2O_3) are vital to achieving the best catalytic performance. However, few studies involving parameter screening have been carried out [8].

Herein we analyse the influence of reforming temperature, steam to carbon molar ratio (S/C) and gas hourly space velocity (GHSV) on the toluene reforming performance. These are considered the key parameters to fine-tune the reaction and maximise the overall performance.

Parallel reactions in this system can be numerous. The main reactions that can occur during toluene steam reforming are represented as follows:

Toluene steam reforming

$$C_7H_8 + 14\,H_2O \rightarrow 7CO_2 + 18\,H_2 \tag{1}$$

$$C_7H_8 + 7\,H_2O \rightarrow 7CO + 11\,H_2 \tag{2}$$

Water–gas shift

$$CO + H_2O \leftrightarrow CO_2 + H_2 \tag{3}$$

Hydrodealkylation

$$C_7H_8 + H_2 \rightarrow C_6H_6 + CH_4 \tag{4}$$

Methane steam reforming

$$CH_4 + H_2O \leftrightarrow CO + 3H_2 \tag{5}$$

Boudouard reaction

$$2CO \leftrightarrow CO_2 + C \tag{6}$$

Steam reforming of toluene is irreversible and Reactions (1) and (2) are dependent on the S/C ratio used. CH_4 is produced from hydroalkylation (Reaction (4)) and pyrolysis of toluene. Methane reforming followed by a water–gas shift reaction converts the produced CO with steam to H_2 and CO_2. A Boudouard reaction is an exothermic reaction that produces C from CO. All of these reactions are heavily conditioned by the temperature, space velocity and reactants ratio [26–28]. Hence, a careful assessment of the impact of these parameters will allow us to identify the optimum conditions towards the generation of added value products.

For all the above, this work fills an essential gap in tar reforming literature via the systematic study of key reaction parameters using a state-of-the-art catalyst to reveal the optimum process conditions.

2. Experimental

2.1. Catalyst Preparation

The nickel-based catalyst was prepared following a wet impregnation method. The necessary amount of $Ni(NO_3)_2 \cdot 6H_2O$ ($\geq 97.0\%$, Sigma-Aldrich) to obtain 20 wt.% NiO was dissolved in an excess of acetone ($\geq 99.8\%$, Sigma Aldrich). Then, the support γ- Al_2O_3 ($\geq 98.0\%$ purity, Sasol) was added into the solution and, after stirring for 2 h, the solvent was removed under vacuum at 60 °C by using a rotating evaporator. The remaining mixture was dried overnight at 110 °C. Finally, the solid was calcined at 600 °C with a ramping rate of 2 °C·min^{-1} for 4 h. It has been reported that Ni/Al_2O_3 catalysts are stable under reaction conditions despite the calcination temperature being lower than those of the experiments [29,30]. Lower calcination temperatures have been shown to lead to better catalytic performance in steam reforming [31]. The obtained sample was labelled Ni/Al_2O_3. The Ni content assuming complete reduction from NiO to Ni is 16.4 wt.%.

2.2. Characterisation

Thermogravimetric analysis (TGA) was carried out to investigate the coke deposition on the catalyst in a Pyris 1 thermogravimetric analyser from PerkinElmer (Waltham, MA, USA). The samples were ramped from room temperature to 900 °C at a rate of 10 °C·min^{-1} in air.

N_2-adsorption-desorption analysis was conducted in a TriStar 3000 V6.07 A analyser from Micromeritics (Norcross, GA, USA). Before the analysis, the catalyst was degassed at 150 °C for 4 h in a vacuum. The Brunauer–Emmett–Teller (BET) method was used to calculate the surface area of the catalyst.

2.3. Catalytic Toluene Steam Reforming Tests

Toluene steam reforming was carried out in a fixed bed reactor used in previous bio-oil reforming work [24]. Before the reaction, the reactor was purged with N_2 to remove air. The catalyst was reduced under 50 mL·min^{-1} of H_2 up to 700 °C for 1 h before each test.

Figure 1 shows the schematic diagram of the experimental reaction set-up, and the reaction zone is shown in Figure 2. The reactor was heated up by two copper electrodes; toluene and steam were injected by two syringe pumps from the top of the reactor and preheated at 200 °C to the vapour phase in a preheating chamber. Toluene was carried by N_2 with a fixed concentration of 100 g Nm^{-3}. Then the reactant stream entered an incoloy alloy 625 tube (12 mm i.d., 2 mm thick, 253 mm long), equipped with an inner quartz tube (9 mm i.d., 1 mm thick, 300 mm long) to prevent any contact between the reactant gas stream and the incoloy internal surface. 500 mg of Ni/Al_2O_3 catalyst with a

particle size in the range of 250–500 µm was placed right in the middle of the quartz tube. A K-type thermocouple was used to determine the catalytic bed temperature.
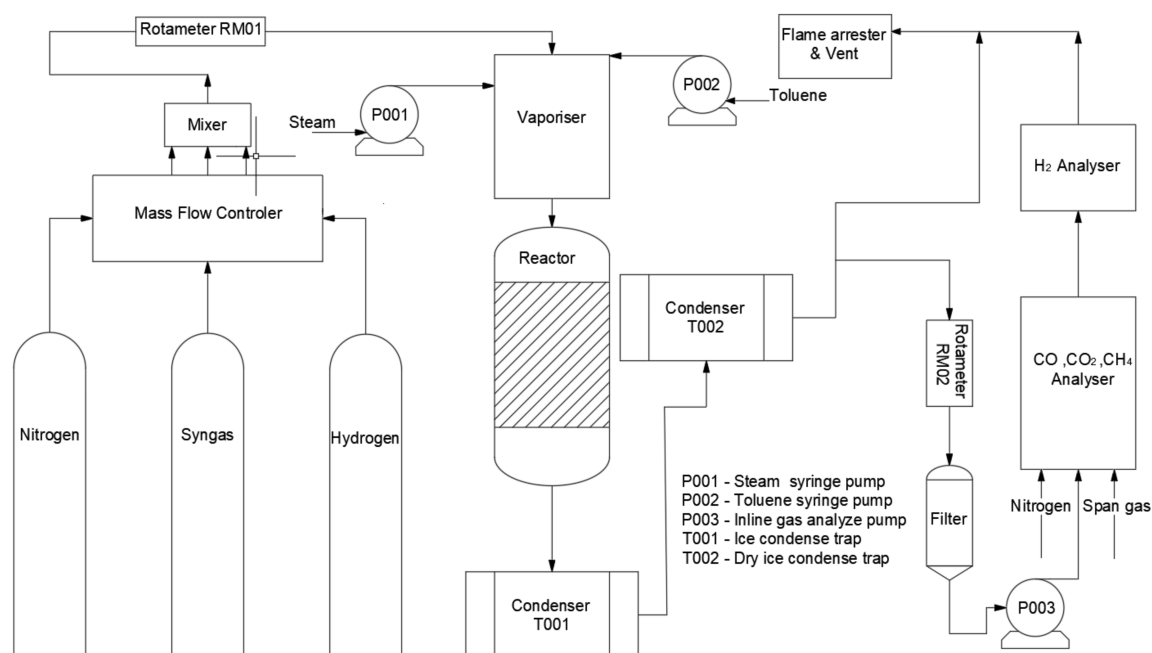

Figure 1. Schematic diagram of the catalytic toluene steam reforming system.

The product gases after reaction pass through two condensers in series to collect any liquid product as well as unreacted toluene and water. Ice and dry ice were used as coolant in the two condensers, respectively. The products identified in the gas phase were H_2, CH_4, CO_2 and CO. Two on-line gas analysers were used to determine the product gas compositions: an MGA3000 Multi-Gas infrared analyser (ADC Gas Analysis, Herts, UK) for CO_2, CH_4 and CO, followed by a K1550 thermal conductivity H_2 analyser (Hitech Instruments, Luton, UK).

The performance of catalysts was evaluated by the conversion into gaseous products (based on a carbon balance between the inlet and the outlet stream of the reactor), selectivity to main products (where "i" is CO_2, CO and CH_4 in moles) and hydrogen yield, which were defined as follows:

$$\% \text{ Carbon Conversion} = \frac{\text{C in the gas product}}{\text{C fed into reactor}} * 100 \tag{7}$$

$$\% \text{ "i" selectivity} = \frac{\text{"i" produced in moles}}{\text{C atoms in the gas products}} * 100 \tag{8}$$

$$\text{Hydrogen yield} = \frac{\text{total Hydrogen production in moles}}{\text{toluene fed into reactor in moles}} \tag{9}$$

The experimental error in toluene conversion, gas selectivity and gas yield is ±2%. Toluene conversion and H_2 production could be influenced by experiment conditions and parameters. Reforming temperature, S/C ratio and residence time are reported to be the key factors that would affect the total conversion and H_2 yield. In this paper S/C ratios of 1, 2 and 3; temperatures of 700, 800 and 900 °C, and GHSV of 30,600, 61,200, 91,800 and 122,400 h^{-1} were investigated.
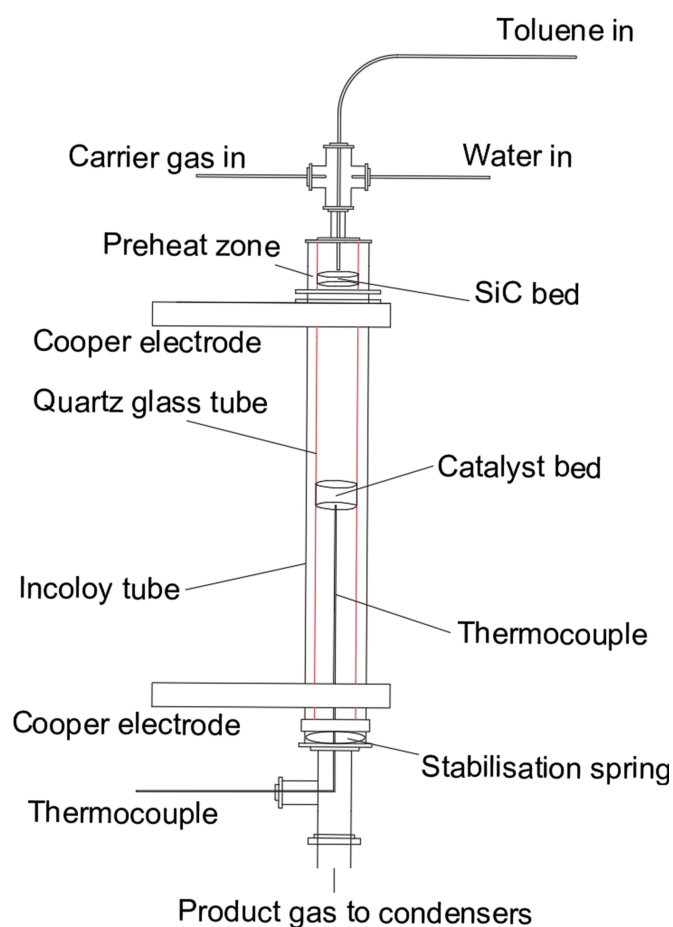
Figure 2. Reactor diagram of catalytic toluene steam reforming.

2.4. Thermodynamic Simulation

The ASPEN software package (AspenTech, Bedford, MA, USA) was used to determine the thermodynamic equilibrium of the toluene reforming reactions over the different reaction conditions. An ideal property method, an RGIBBS reactor (based on Gibbs free energy minimisation) was selected to investigate the thermodynamic equilibrium. Material flows into the reactor are identical to those from the corresponding experiment. The influence and effects of experimental parameters, including reforming the temperature and S/C ratio on the toluene conversion, the yield of main light gases and the carbon deposition was investigated.

3. Results and Discussion

3.1. Textural Properties of the Synthetised Catalyst

The N_2 adsorption-desorption isotherm of the calcined Ni/Al_2O_3 catalyst is shown in Figure 3, which shows a type IV isotherm with a characteristic hysteresis loop for mesoporous materials. The adsorption average pore width was 9.1 nm, the total pore volume was 0.35 $cm^3 \cdot g^{-1}$ and BET Surface Area was 153 $m^2 \cdot g^{-1}$. The BET surface area, pore volume and pore width of the original Al_2O_3 was 230 $m^2 \cdot g^{-1}$, 0.5 $cm^3 \cdot g^{-1}$ and 10 nm respectively. Textural properties are actually governed by the primary support gamma-alumina, which provides mechanical and thermal stability as well as high surface area.
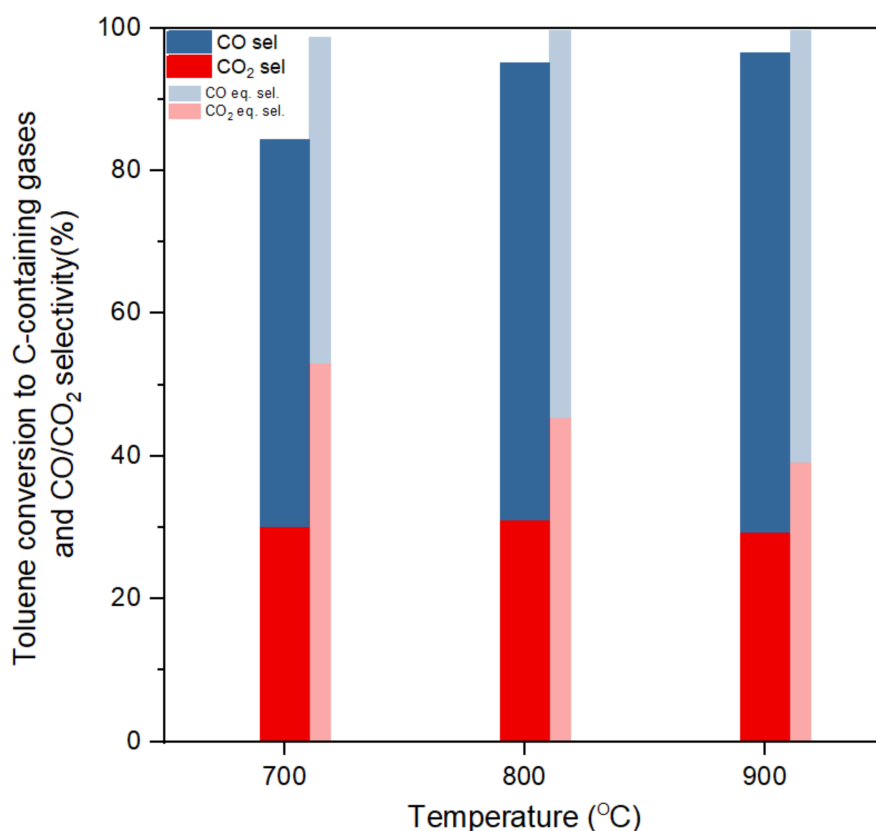
Figure 3. Toluene conversion to C-containing gases and CO/CO_2 selectivity at different temperatures (S/C:3, gas hourly space velocity (GHSV):61,200 h^{-1}).

3.2. Influence of Temperature on Toluene Steam Reforming

The steam reforming temperature was concluded to have a significant influence on toluene conversion since higher temperatures could increase syngas production and conversion from toluene to gas products [32]. When reforming is envisaged as a downstream tar upgrading unit after gasification, the most interesting temperature interval for atmospheric reforming is between 600 and 900 °C, since the gasification effluent temperature will normally be lower than 900 °C [33]. Research also suggested that high temperature might reduce H$_2$ yield as the reverse water–gas shift reaction is favoured due to its endothermic nature [34–36]. The experiments were conducted at different temperatures to investigate the most suitable conditions for toluene conversion and H$_2$ production. Catalytic performance tests were performed at 700, 800 and 900 °C, with a fixed S/C ratio of 3 and a GHSV of 61,200 h^{-1} (corresponding to a N$_2$ flow rate of 300 mL·min^{-1}) for 5 h.

Figure 3 shows the toluene conversion and CO_2/CO selectivity (based on conversion to C-containing gases) at the three different temperatures in a steady state within the five hours of reaction and compares with equilibrium selectivity. CO and CO_2 were the main gases. The experimental selectivity of CH$_4$ at all temperatures was under 0.1%. Conversion and selectivity of the gases approached that of thermodynamic equilibrium as temperature increased. Thermodynamic equilibrium predicts total toluene conversion at 700 °C or higher temperatures. At 700 °C, the thermodynamic equilibrium indicated a CH$_4$ selectivity of 1.1%, and for higher temperatures only CO and CO_2 were predicted as C-containing gas products. Experimental toluene conversions ranged from 84% to 96% and approached equilibrium with the temperature increase from 700 to 900 °C. Coke formation only accounted for less than 1% of toluene conversion, the rest being to gas phase products. Unreacted toluene was condensed in the cooling trap, which enabled closing the mass balance within 98%. The high conversions of toluene achieved for the three temperatures highlight once again the good performance of this commercial-like

catalyst (Ni/Al_2O_3). Both experimental and equilibrium selectivity showed that the CO/CO_2 ratio increases as temperature increases. This is likely dominated by a reverse water–gas shift reaction in the high-temperature area (Reaction (3), as the increasing temperature would favour the endothermic direction, and nickel contents would also promote the reaction at high temperatures [11].

Table 1 shows the gaseous product yields including CO, CO_2, H_2 and CH_4. The yields of CO and CO_2 have similar trends to selectivity. However, for H_2 yield the maximum was achieved at 800 °C with a H_2 production of 13.0 mol/mol toluene, while the highest H_2 production in equilibrium conditions was predicted at 700 °C. This can be due to, in the experimental test at 700 °C, the lowest toluene conversion into gases was obtained. Toluene conversion to gas stayed over 94% at 800 °C or above, while a higher temperature would lead to a slight decrease in the content of H_2 in gaseous products due to the presence of the reverse water–gas shift reaction as discussed above. It is interesting to remark that only at 700 °C the undesirable CH_4 side product was obtained and it was only in a small amount. The absence of CH_4 at higher temperatures can be due to the methane reforming to CO and other parallel processes consuming methane as suggested by the equilibrium results.

Table 1. Product yields for the gaseous products at the three different temperatures (S/C:3, GHSV: 61,200 h^{-1}).

Temperature (°C)	CO_2 (mol/mol Toluene)	CO (mol/mol Toluene)	H_2 (mol/mol Toluene)	CH_4 (mol/mol Toluene)
700	2.1	3.8	10.3	0
(equilibrium)	(3.7)	(3.2)	(14.5)	(0.1)
800	2.2	4.5	13.0	0
(equilibrium)	(3.2)	(3.8)	(14.3)	(0)
900	2.1	4.7	11.8	0
(equilibrium)	(2.8)	(4.2)	(13.8)	(0)

Thermogravimetric analysis was conducted on the catalysts after a five-hour reaction to estimate the coke formation during the three different temperatures reaction tests. It has been reported that coke deposition on Ni/Al_2O_3 catalysts is the main cause for deactivation and high nickel contents could also favour coke formation. Although coke deposition is thermodynamically unfavourable at high temperatures (>600 °C), methane decomposition in the high temperature range could lead to the production of solid carbon [37]. Table 2 shows the carbon conversion from toluene to coke and the fraction of coke on the catalyst as a function of temperature. As the temperature increased, the conversion to carbon deposits was slightly higher. It is likely that carbon at the higher temperatures was formed from the reforming of CH_4 observed at lower temperatures, as CH_4 is known to favour coke formation on Ni-based catalysts [27]. Notwithstanding coke formation at these temperatures, the amount of coke is very low, and the catalyst remains stable during the whole experiment.

Table 2. Toluene conversion to coke and fraction of coke deposited on the catalyst at different reforming temperatures (S/C:3, GHSV:61,200 h^{-1}, 5-h test).

Reforming Temperature	700 °C	800 °C	900 °C
Coke/C in toluene	0.43%	0.61%	0.77%
Coke/Catalyst (g_C/g_{cat})	0.118	0.167	0.211

Based on the results presented above, 800 °C was considered the most suitable reforming temperature due to the highest H_2 production, an excellent overall conversion (94%) and acceptable coke deposition levels. On the contrary, despite the 900 °C experiment showing a slightly higher toluene conversion, lower H_2 production, greater coke deposition and lower energy efficiency made this temperature not preferable with the 800 °C test.

Gas analysis as a function of time on stream at the chosen temperature is shown in Figure 4 for a five-hour test. There was no CH_4 detected throughout the test and CO, CO_2 and H_2 concentration stayed stable *ca* 11%, 23% and 66% (figures corrected from N_2 dilution), respectively, during the whole experiment. Furthermore, no obvious change in the CO/CO_2 ratio, or drop in H_2 yields and catalyst deactivation were observed in this test.
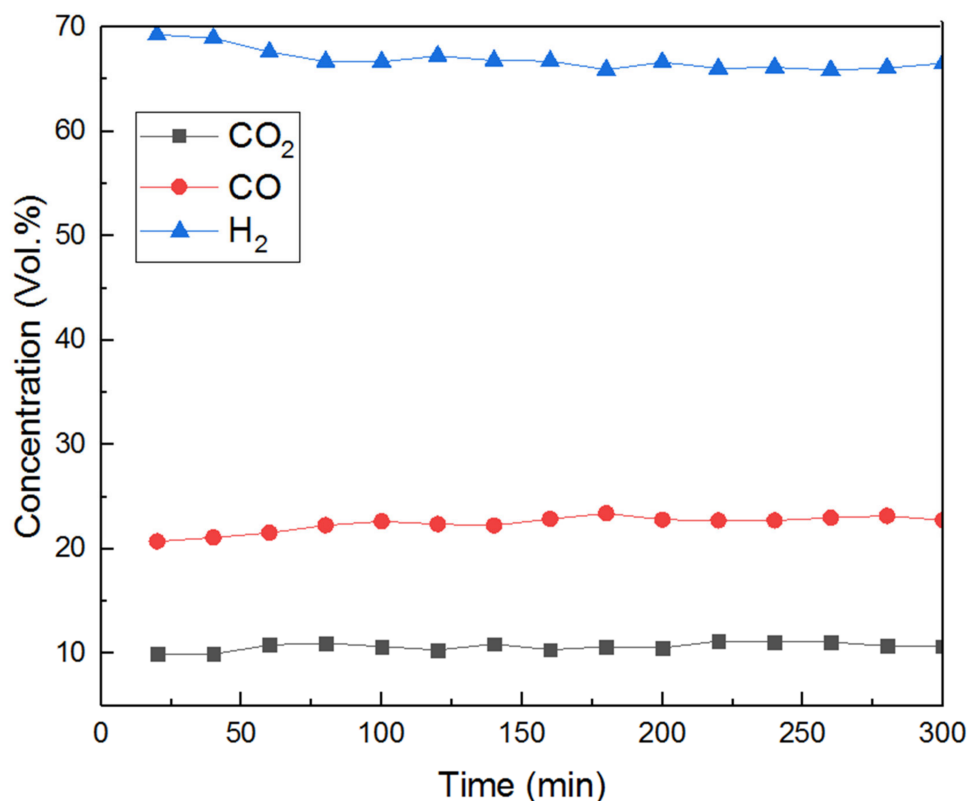

Figure 4. Gas product concentration at 800 °C, S/C:3, GHSV:61,200 h^{-1} in a 5-h test.

3.3. Influence of GHSV in Toluene Steam Reforming

In view of the results obtained in the temperature screening, a temperature of 800 °C was chosen to study the effect of GHSV to elucidate the suitable residence time for a complete conversion of toluene. High GHSV, or lower residence time, might inhibit toluene conversion and H_2 production. Literature suggests that suitable GHSVs for steam reforming were mostly between 10,000 and 70,000 h^{-1} [38,39] over different catalysts. For our benchmark catalyst, tests were carried out with 500 mg of catalyst, and a fixed temperature (800 °C) and S/C ratio of three during 5 h of reaction. The feeding rates of toluene, steam and N_2 were changed according to the desired GHSV. The GHSV studied were 30,600, 61,200, 91,800 and 122,400 h^{-1}. Some of the space velocities selected in this study are indeed over the standard ranges mentioned above. In fact, high space velocities normally involve lower reactor volumes, thus decreasing the capital cost of the reformer.

Figure 5 shows the toluene conversion and CO_2/CO selectivity (based on conversion to C-containing gases) at the four different GHSVs in a steady state within the five hours of reaction and compares them with equilibrium selectivity. Toluene conversion decreased from 96% to 86% when GHSVs increased from 30,600 to 122,400 h^{-1}. When GHSV was 91,800 h^{-1} or lower, toluene conversion to gas remained higher than 90%, without notorious differences for the two lowest GHSV studied (30,600 h^{-1} or 61,200 h^{-1}), which showed a stabilised conversion at around 95%. The selectivity of CO and CO_2 approached the equilibrium results slowly when GHSV decreased. It could be seen that toluene conversion and CO_2 selectivity declined with the increasing of GHSV, as a result of shorter residence time and reaction period. It is interesting to note that the selectivity is less affected by the residence

time than the conversion. Negligible or no methane was detected in the product gas, which was in line with literature that suggested that at temperatures higher than 750 °C very small amounts of CH_4 are produced [11].
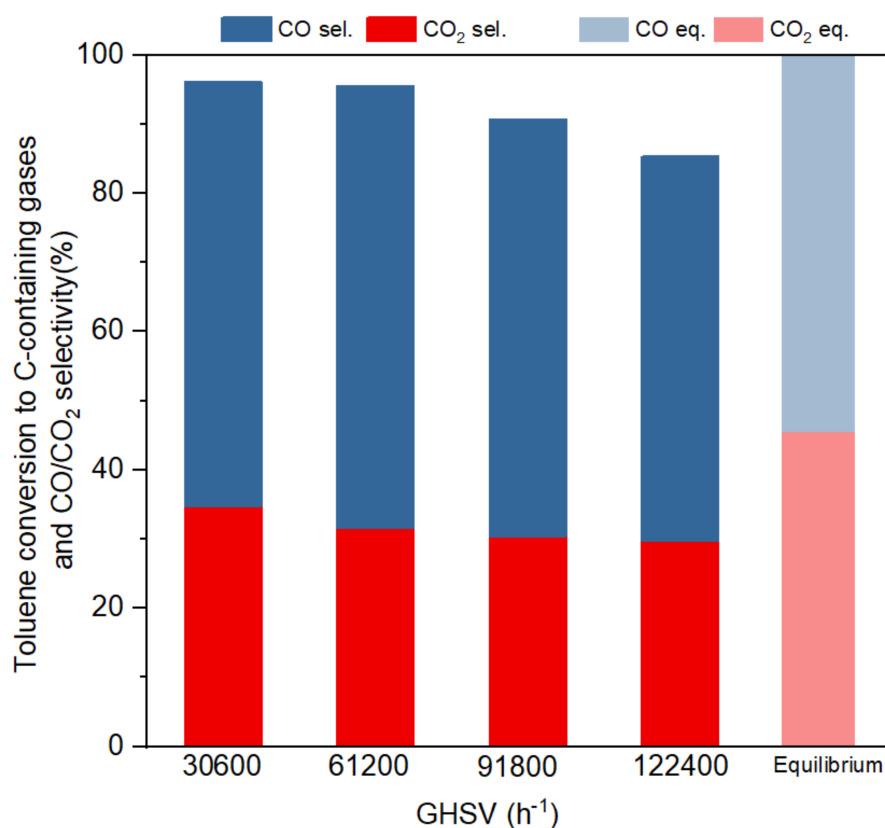

Figure 5. Toluene conversion to C-containing gases and CO/CO_2 selectivity at different GHSVs (S/C:3, 800 °C).

The gas product CO_2, CO and H_2 yields are shown in Table 3. As expected, GHSV 30,600 h^{-1} led to the highest H_2 production (13.2 mol/mol toluene). As a trend, CO, CO_2 and H_2 yields dropped when GHSV increased. This decrease in yields for all gas products at high GHSV is linked with the drop in conversion as the residence time became shorter. An exception occurred at 61,200 h^{-1} GHSV as the reverse water–gas shift reaction could cause a small increase in CO. Previous studies suggest that some tar model compounds (naphthalene) had no apparent trends for the hydrogen yields or selectivity, as the product was affected by the equilibrium of the water–gas shift reaction and other side reactions [40]. In this work, hydrogen yield and total conversion showed a slightly increasing trend in conversion and yields with the decrease of residence time, but this trend was more remarkable in the conversion of toluene than in selectivities.

Table 3. Product yields for the gaseous products at different GHSV (S/C:3, 800 °C).

GHSV (h^{-1})	CO_2 (mol/mol Toluene)	CO (mol/mol Toluene)	H_2 (mol/mol Toluene)
30,600	2.4	4.3	13.2
61,200	2.2	4.5	13.0
91,800	2.1	4.2	12.8
122,400	2.1	3.9	10.8
(Equilibrium)	(3.2)	(3.8)	(14.3)

Table 4 shows the carbon conversion from toluene to coke with different GHSVs. This data led us to a better understanding of the coke deposition. The reactant toluene and steam feeding rate increased three times when GHSV increased from 30,600 to 122,400 h^{-1}; however, the coke conversion reduced from 0.38% to 0.22%. This means that the higher GHSV used resulted in a higher coke amount deposited but lower conversion rate. This result is the balance between the higher feed of toluene used and the decrease in conversion due to the high GHSV used.

Table 4. Toluene conversion to coke deposited on the catalyst with different GHSV (S/C:3, 800 °C, five-hour test).

GHSV(h^{-1})	30,600	61,200	91,800	122,400
Coke/C in toluene	0.38%	0.31%	0.23%	0.22%
Coke/Catalyst (g$_C$/g$_{cat}$)	0.105	0.167	0.188	0.242

Although the lower space velocity leads to higher conversion, greater selectivity and the lower net amount of carbon deposits, for practical applications (i.e. manufacturing cost savings) higher space velocities are desired. In this sense, 61,200 h^{-1} yields very similar conversion and selectivity levels, low net coking and lower conversion to coke. Hence, this space velocity was selected to optimise the next reaction parameter.

3.4. Influence of S/C Ratio in Toluene Steam Reforming

Steam, as a principal reactant in catalytic steam reforming, is widely recognised to have a strong influence on H$_2$ production. Steam is involved in most of the relevant reactions in the toluene reforming and therefore the steam to carbon ratio was chosen as a key variable to study. A high steam partial pressure improves gasification reactions and moves the water–gas shift equilibrium towards hydrogen production, while the partial pressure of toluene in the gas stream is lower due to dilution as the S/C ratio rises [37]. Suitable S/C ratios to investigate the catalyst performance were mostly between one and four in the literature [16,41]. Although steam is the main reactant in a reforming process, a large excess of water in these experiments could condense into ice in the cooling trap and block the system. It is also reported that the saturation of the catalyst surface by steam at a high S/C ratio would not favour the conversion of toluene or H$_2$ production [5].

In this study, the catalytic performance tests were performed at three different S/C ratios of 1, 2, 3, at 800 °C, 500 mg of samples and a GHSV of 61,200 h^{-1} for five hours.

Figure 6 shows the influence of the S/C ratio on the selectivity of carbon containing products. Both experimental and equilibrium results showed that an increment in S/C ratio results in a large improvement of CO$_2$ selectivity and toluene conversion. In the experimental tests, toluene to gas conversion increased from 53% to 94% when the S/C ratio increased from one to three. Equilibrium results indicated that a higher S/C ratio always increases the H$_2$ production, as the excess steam would promote the water–gas shift reaction. A higher S/C ratio also increased toluene conversion to gas. Some researchers suggested that the most suitable S/C ratio was mostly between 2.5 and 3.5, because more excess steam would not increase toluene conversion or H$_2$ production, causing a drop in toluene partial pressure [26].

Table 5 compares the product yields of CO, CO$_2$ and H$_2$ with different S/C ratios. Equilibrium simulation and experiments both showed large increases in CO$_2$ and H$_2$ production with the S/C ratio. Experimental H$_2$ yield increased from 5.1 to 13.0 mol/mol toluene when the S/C ratio raised from one to three. The opposite equilibrium trend is expected for CO, but this did not happen in the experiments. Instead, the CO yield was observed to increase with the amount of steam as the trend was dominated by the higher conversion achieved at higher S/C ratios. Despite the experimental CO yield showing a slight increase, in general the CO/CO$_2$ ratio decreased with the increase of the S/C ratio in line with the equilibrium results.
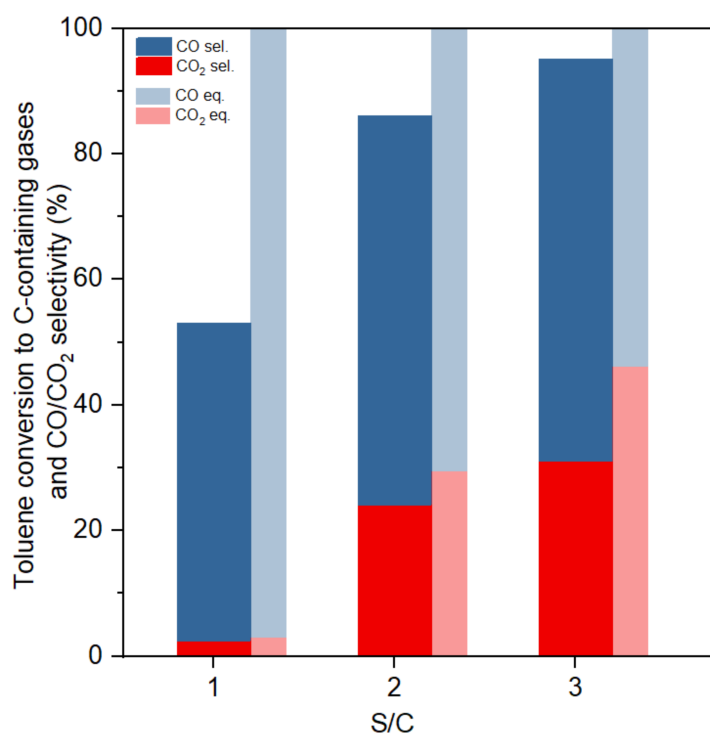
Figure 6. Toluene conversion to C-containing gases and CO/CO$_2$ selectivity at different S/C ratios (GHSV:61,200 h^{-1}, 800 °C).

Table 5. Product yields for the gaseous products under different S/C ratios (GHSV:61,200 h^{-1}, 800 °C).

S/C ratio	CO$_2$ (mol/mol Toluene)	CO (mol/mol Toluene)	H$_2$ (mol/mol Toluene)
1	0.2	3.5	5.1
(Equilibrium)	(0.2)	(6.8)	(9.8)
2	1.7	4.3	10.5
(Equilibrium)	(2.1)	(4.9)	(13.0)
3	2.2	4.5	13.0
(Equilibrium)	(3.2)	(3.8)	(14.3)

The coke weight on the spent catalyst with S/C ratio 1, 2, 3 is 0.289, 0.222, 0.167 g$_C$/g$_{cat}$, respectively. As expected, the higher S/C ratio promoted carbon gasification avoiding coke formation [42]. Table 6 shows the carbon conversion from toluene to coke for the three different S/C ratio studied. As discussed above, it can be seen that the excess of steam inhibited, but did not suppress, the formation of coke. For all the above, the better choice is to use a S/C ratios of three since it permits the highest H$_2$ production and toluene conversion and the lowest coke amount.

Table 6. Toluene conversion to coke deposited on the catalyst at different S/C ratios.

S/C ratio	1	2	3
Coke/C in toluene	1.07%	0.82%	0.61%
Coke/Catalyst (g$_C$/g$_{cat}$)	0.289	0.222	0.167

4. Conclusions

To remove tar produced from biomass gasification, catalytic steam reforming was conducted for toluene as a model tar compound. Simulations of a thermodynamic equilibrium based on Gibbs free energy minimisation and experiments in a fixed bed reactor using a Ni/Al$_2$O$_3$ catalyst were carried

out. The effect of reforming temperature, S/C ratio and GHSV on toluene conversion and product distribution was studied.

Increasing the temperature from 700 to 900 °C increased total conversion, with a potential risk of higher coke deposition. A temperature of 800 °C observed the highest H_2 production, high toluene conversion (>94%) and relatively lower coke deposition.

The Ni/Al_2O_3 catalyst only requires a very short residence time (GHSV < 91,800 h^{-1}) for toluene reforming with this catalyst and effectively removes low density toluene in a mixed gas stream. H_2 yield and toluene conversion increased slightly and approached simulated thermodynamic equilibrium results when GHSV decreased. Coke deposition increased at a lower rate as GHSV increased.

A high S/C ratio would greatly increase total conversion, hydrogen production and reduce the coke formation on the catalyst. The presence of excess steam could shift the equilibrium of the water–gas shift reaction to produce more H_2.

A temperature of 800 °C, GHSV of 61,200 h^{-1} and S/C ratio of three provided the most suitable reaction conditions for toluene conversion and H_2 production in steam reforming of toluene, obtained a steady state of a toluene to gas conversion over 94%, a H_2 production of 141.6 mol/mol toluene in a five-hour test, with no obvious deactivation observed in five hours. Based on these results, this condition would be suitable for tar model compound removal.

References

1. Farzad, S.; Mandegari, M.A.; Görgens, J.F. A critical review on biomass gasification, co-gasification, and their environmental assessments. *Biofuel Res. J.* **2016**, *3*, 483–495. [CrossRef]
2. Göransson, K.; Söderlind, U.; He, J.; Zhang, W. Review of syngas production via biomass DFBGs. *Renew. Sustain. Energy Rev.* **2011**, *15*, 482–492. [CrossRef]
3. International Energy Agency. *International Energy Outlook 2017*; International Energy Agency: Paris, France, 2017.
4. Balat, H.; Kırtay, E. Hydrogen from biomass–present scenario and future prospects. *Int. J. Hydrogen Energy* **2010**, *35*, 7416–7426. [CrossRef]
5. Świerczyński, D.; Libs, S.; Courson, C.; Kiennemann, A. Steam reforming of tar from a biomass gasification process over Ni/olivine catalyst using toluene as a model compound. *Appl. Catal. B-Environ.* **2007**, *74*, 211–222. [CrossRef]
6. Claude, V.; Mahy, J.G.; Douven, S.; Pirard, S.L.; Courson, C.; Lambert, S.D. Ni-and Fe-doped γ-Al_2O_3 or olivine as primary catalyst for toluene reforming. *Mater. Today Chem.* **2019**, *14*, 100197. [CrossRef]
7. Devi, L.; Ptasinski, K.J.; Janssen, F.J. A review of the primary measures for tar elimination in biomass gasification processes. *Biomass Bioenergy* **2003**, *24*, 125–140. [CrossRef]
8. Anis, S.; Zainal, Z.A. Tar reduction in biomass producer gas via mechanical, catalytic and thermal methods: A review. *Renew. Sustain. Energy Rev.* **2011**, *15*, 2355–2377. [CrossRef]
9. Noichi, H.; Uddin, A.; Sasaoka, E. Steam reforming of naphthalene as model biomass tar over iron–aluminum and iron–zirconium oxide catalyst catalysts. *Fuel Process. Technol.* **2010**, *91*, 1609–1616. [CrossRef]
10. Guan, G.; Kaewpanha, M.; Hao, X.; Abudula, A. Catalytic steam reforming of biomass tar: Prospects and challenges. *Renew. Sustain. Energy Rev.* **2016**, *58*, 450–461. [CrossRef]
11. Zhao, B.; Zhang, X.; Chen, L.; Qu, R.; Meng, G.; Yi, X.; Sun, L. Steam reforming of toluene as model compound of biomass pyrolysis tar for hydrogen. *Biomass Bioenergy* **2010**, *34*, 140–144. [CrossRef]
12. Virginie, M.; Courson, C.; Kiennemann, A. Toluene steam reforming as tar model molecule produced during biomass gasification with an iron/olivine catalyst. *Comptes Rendus Chimie* **2010**, *13*, 1319–1325. [CrossRef]

13. Park, H.J.; Park, S.H.; Sohn, J.M.; Park, J.; Jeon, J.K.; Kim, S.S.; Park, Y.K. Steam reforming of biomass gasification tar using benzene as a model compound over various Ni supported metal oxide catalysts. *Bioresour. Technol.* **2010**, *101*, S101–S103. [CrossRef] [PubMed]

14. Lorente, E.; Millan, M.; Brandon, N.P. Use of gasification syngas in SOFC: Impact of real tar on anode materials. *Int. J. Hydrogen Energy* **2012**, *37*, 7271–7278. [CrossRef]

15. Lorente, E.; Berrueco, C.; Millan, M.; Brandon, N.P. Effect of tar fractions from coal gasification on nickel-yttria stabilized zirconia and nickel-gadolinium doped ceria solid oxide fuel cell anode materials. *J. Power Sources* **2013**, *242*, 824–831. [CrossRef]

16. Coll, R.; Salvado, J.; Farriol, X.; Montane, D. Steam reforming model compounds of biomass gasification tars: Conversion at different operating conditions and tendency towards coke formation. *Fuel Process. Technol.* **2001**, *74*, 19–31. [CrossRef]

17. Matsumura, Y.; Nakamori, T. Steam reforming of methane over nickel catalysts at low reaction temperature. *Appl. Catal. A-Gen.* **2004**, *258*, 107–114. [CrossRef]

18. Lertwittayanon, K.; Youravong, W.; Lau, W.J. Enhanced catalytic performance of Ni/α-Al$_2$O$_3$ catalyst modified with CaZrO$_3$ nanoparticles in steam-methane reforming. *Int. J. Hydrogen Energy* **2017**, *42*, 28254–28265. [CrossRef]

19. Ahmed, T.; Xiu, S.; Wang, L.; Shahbazi, A. Investigation of Ni/Fe/Mg zeolite-supported catalysts in steam reforming of tar using simulated-toluene as model compound. *Fuel* **2018**, *211*, 566–571. [CrossRef]

20. Mermelstein, J.; Millan, M.; Brandon, N.P. The impact of carbon formation on Ni–YSZ anodes from biomass gasification model tars operating in dry conditions. *Chem. Eng. Sci.* **2009**, *64*, 492–500. [CrossRef]

21. Xu, H.; Liu, Y.; Sun, G.; Kang, S.; Wang, Y.; Zheng, Z.; Li, X. Synthesis of graphitic mesoporous carbon supported Ce-doped nickel catalyst for steam reforming of toluene. *Mater. Lett.* **2019**, *244*, 123–125. [CrossRef]

22. Li, Z.; Li, M.; Ashok, J.; Kawi, S. NiCo@ NiCo phyllosilicate@ CeO$_2$ hollow core shell catalysts for steam reforming of toluene as biomass tar model compound. *Energy Convers. Manag.* **2019**, *180*, 822–830. [CrossRef]

23. Ashok, J.; Dewangan, N.; Das, S.; Hongmanorom, P.; Wai, M.H.; Tomishige, K.; Kawi, S. Recent progress in the development of catalysts for steam reforming of biomass tar model reaction. *Fuel Process. Technol.* **2020**, *199*, 106252. [CrossRef]

24. Bizkarra, K.; Bermudez, J.M.; Arcelus-Arrillaga, P.; Barrio, V.L.; Cambra, J.F.; Millan, M. Nickel based monometallic and bimetallic catalysts for synthetic and real bio-oil steam reforming. *Int. J. Hydrogen Energy* **2018**, *43*, 11706–11718. [CrossRef]

25. Meng, J.; Zhao, Z.; Wang, X.; Wu, X.; Zheng, A.; Huang, Z.; Li, H. Effects of catalyst preparation parameters and reaction operating conditions on the activity and stability of thermally fused Fe-olivine catalyst in the steam reforming of toluene. *Int. J. Hydrogen Energy* **2018**, *43*, 127–138. [CrossRef]

26. Oh, G.; Park, S.Y.; Seo, M.W.; Kim, Y.K.; Ra, H.W.; Lee, J.G.; Yoon, S.J. Ni/Ru–Mn/Al$_2$O$_3$ catalysts for steam reforming of toluene as model biomass tar. *Renew. Energy* **2016**, *86*, 841–847. [CrossRef]

27. Meidanshahi, V.; Bahmanpour, A.M.; Iranshahi, D.; Rahimpour, M.R. Theoretical investigation of aromatics production enhancement in thermal coupling of naphtha reforming and hydrodealkylation of toluene. *Chem. Eng. Process* **2011**, *50*, 893–903. [CrossRef]

28. Tang, Y.; Liu, J. Effect of anode and Boudouard reaction catalysts on the performance of direct carbon solid oxide fuel cells. *Int. J. Hydrogen Energy* **2010**, *35*, 11188–11193. [CrossRef]

29. Zhang, Y.; Williams, P.T. Carbon nanotubes and hydrogen production from the pyrolysis catalysis or catalytic-steam reforming of waste tyres. *J. Anal. Appl. Pyrol.* **2016**, *122*, 490–501. [CrossRef]

30. Yue, B.; Wang, X.; Ai, X.; Yang, J.; Li, L.; Lu, X.; Ding, W. Catalytic reforming of model tar compounds from hot coke oven gas with low steam/carbon ratio over Ni/MgO–Al2O3 catalysts. *Fuel Process. Technol.* **2010**, *91*, 1098–1104. [CrossRef]

31. Dieuzeide, M.L.; Iannibelli, V.; Jobbagy, M.; Amadeo, N. Steam reforming of glycerol over Ni/Mg/γ-Al2O3 catalysts. Effect of calcination temperatures. *Int. J. Hydrogen Energy* **2012**, *37*, 14926–14930. [CrossRef]

32. Bona, S.; Guillén, P.; Alcalde, J.G.; García, L.; Bilbao, R. Toluene steam reforming using coprecipitated Ni/Al catalysts modified with lanthanum or cobalt. *Chem. Eng. J.* **2008**, *137*, 587–597. [CrossRef]

33. Quitete, C.P.; Bittencourt, R.C.P.; Souza, M.M. Steam reforming of tar using toluene as a model compound with nickel catalysts supported on hexaaluminates. *Appl. Catal. A-Gen.* **2014**, *478*, 234–240. [CrossRef]

34. Yang, L.; Pastor-Pérez, L.; Gu, S.; Sepúlveda-Escribano, A.; Reina, T.R. Highly efficient Ni/CeO$_2$-Al$_2$O$_3$ catalysts for CO$_2$ upgrading via reverse water-gas shift: Effect of selected transition metal promoters. *Appl. Catal. B-Environ.* **2018**, *232*, 464–471. [CrossRef]

35. Zhu, H.L.; Zhang, Y.S.; Materazzi, M.; Aranda, G.; Brett, D.J.; Shearing, P.R.; Manos, G. Co-gasification of beech-wood and polyethylene in a fluidized-bed reactor. *Fuel Process. Technol.* **2019**, *190*, 29–37. [CrossRef]

36. Stroud, T.; Smith, T.J.; Le Saché, E.; Santos, J.L.; Centeno, M.A.; Arellano-Garcia, H.; Odriozola, J.A.; Reina, T.R. Chemical CO$_2$ recycling via dry and bi reforming of methane using Ni-Sn/Al$_2$O$_3$ and Ni-Sn/CeO$_2$-Al$_2$O$_3$ catalysts. *Appl. Catal. B-Environ.* **2018**, *224*, 125–135. [CrossRef]

37. Mukai, D.; Tochiya, S.; Murai, Y.; Imori, M.; Hashimoto, T.; Sugiura, Y.; Sekine, Y. Role of support lattice oxygen on steam reforming of toluene for hydrogen production over Ni/La$_{0.7}$Sr$_{0.3}$AlO$_3-\delta$ catalyst. *Appl. Catal. A-Gen.* **2013**, *453*, 60–70. [CrossRef]

38. Frusteri, F.; Freni, S.; Spadaro, L.; Chiodo, V.; Bonura, G.; Donato, S.; Cavallaro, S. H2 production for MC fuel cell by steam reforming of ethanol over MgO supported Pd, Rh, Ni and Co catalysts. *Catal. Commun.* **2004**, *5*, 611–615. [CrossRef]

39. He, L.; Hu, S.; Jiang, L.; Liao, G.; Chen, X.; Han, H.; Xiao, L.; Ren, Q.; Wang, Y.; Su, S.; et al. Carbon nanotubes formation and its influence on steam reforming of toluene over Ni/Al$_2$O$_3$ catalysts: Roles of catalyst supports. *Fuel Process. Technol.* **2018**, *176*, 7–14. [CrossRef]

40. Li, Q.; Wang, Q.; Kayamori, A.; Zhang, J. Experimental study and modeling of heavy tar steam reforming. *Fuel Process. Technol.* **2018**, *178*, 180–188. [CrossRef]

41. Li, C.; Hirabayashi, D.; Suzuki, K. Development of new nickel based catalyst for biomass tar steam reforming producing H2-rich syngas. *Fuel Process. Technol.* **2009**, *90*, 790–796. [CrossRef]

42. Le Saché, E.; Pastor-Pérez, L.; Garcilaso, V.; Watson, D.; Centeno, M.A.; Odriozola, J.A.; Reina, T.R. Flexible syngas production using a La$_2$Zr$_2$-xNixO$_7$-δ pyrochlore-double perovskite catalyst: Towards a direct route for gas phase CO$_2$ recycling. *Catal. Today* **2019**. [CrossRef]